

MASS TRANSFER PHENOMENA IN FLUIDIZED BEDS WITH VERTICALLY AND HORIZONTALLY IMMersed MEMBRANES

Ramon VONCKEN, Ivo ROGHAI^{*}, Fausto GALLUCCI and Martin VAN SINT ANNALAND

Chemical Process Intensification, Department of Chemical Engineering and Chemistry, Eindhoven University of Technology, THE NETHERLANDS

^{*}Corresponding author, E-mail address: i.roghair@tue.nl

ABSTRACT

The hydrodynamics and mass transfer phenomena in fluidized bed membrane reactors were studied with an extended version of the OpenFOAM® Two-Fluid Model (TFM). Using a hydrogen-nitrogen gas mixture as fluidizing gas, the membranes were used for in-situ selective hydrogen extraction. The simulation results were compared to experiments. Both vertically and horizontally immersed membranes were simulated as 2-dimensional representations of the experimental set-ups.

The membrane fluxes obtained from vertical membrane simulations are close to the experimental values, the average deviation being 4%. The concentration profiles along the reactor width indicate that concentration polarization is occurring at every gas mixture composition and pressure. Up to 60% of the reactor width is polarized. The polarization increases at higher axial positions in the bed.

Experiments and simulations show the appearance of densified particle zones on top of horizontal membranes and gas pockets underneath the membranes. The densified zones and gas pockets are most pronounced near the walls, which is also where the most pronounced reduction in hydrogen concentrations occurs.

To sum up, both vertical and horizontal membranes show reduced hydrogen concentrations near the membranes. Further simulations at various pressures, concentrations and geometries should be performed to fully compare both configurations and determine their effectivities.

NOMENCLATURE

A	area	[m ²]
C_d	drag coefficient	[-]
D	diffusion coefficient	[m ² /s]
g	gravitational acceleration	[m/s ²]
M	molar weight	[kg/mol]
n	power in Sieverts' law	[-]
p	pressure	[Pa]
Q	membrane permeance	[mol/(m ² .s.Pa ⁿ)]
R	universal gas constant	[J/(mol.K)]
Re	Reynolds number	[-]
S	membrane mass source term	[kg/(m ³ .s)]
t	time	[s]
T	temperature	[K]
\mathbf{u}	velocity	[m/s]
V	volume	[m ³]

X	molar fraction	[-]
Y	mass fraction	[-]
α	hold-up fraction	[-]
β	interphase drag coefficient	[kg/(m ³ .s)]
γ	dissipation of fluctuation energy	[kg/(m.s ³)]
θ	granular temperature	[m ² /s ²]
κ	conductivity of fluctuation energy	[kg/(m.s)]
μ	shear/dynamic viscosity	[Pa.s]
ρ	density	[kg/m ³]
τ	shear stress tensor	[Pa]

c	cell
H_2	hydrogen
g	gas
i	phase
m	membrane
p	particle
ret	retentate
s	solid
sim	simulation
tot	total

INTRODUCTION

A commonly employed method to produce hydrogen is steam reforming of natural gas. Steam Methane Reforming (SMR) can be performed in (multi-tubular) packed bed reactors, in which methane reacts with steam to form carbon mono-oxide and hydrogen. Consecutively, the Water Gas Shift (WGS) reaction occurs; the carbon monoxide reacts with steam to form carbon dioxide and hydrogen. The SMR reaction is endothermic and limited by equilibrium, thus high temperatures and low hydrogen concentrations are required to obtain a high conversion. Furthermore, the CO₂ produced by the WGS reaction is emitted into the atmosphere. Purifying and storing a CO₂ stream from the system will result in an increase in cost and energy usage, and a decrease in performance, see Medrano et al. (2014). A promising approach to reduce cost and energy usage is integrating the separation and reaction steps. Separation of hydrogen from the reaction mixture can be done using modern, high-flux hydrogen selective palladium membranes. Extracting hydrogen draws the equilibrium to the product side and eliminates the need of downstream CO₂ separation steps.

The integration of hydrogen selective membranes in packed bed reactors for hydrogen recovery has already been proposed by e.g. Tsotsis et al. (1992), Han et al.

(1994) and Tiemersma et al. (2006). In these systems, catalysed reactions and separation of product and waste are performed in the same unit. However, a major drawback of packed bed membrane reactors is the low mixing efficiency, causing temperature and concentration gradients in the reactor. This can be detrimental for membrane performance (see Gallucci et al. (2010)) and cause mass transfer limitations between the fluid and particles, and between the fluid and membrane (concentration polarization). Especially state-of-the-art membranes can achieve very high fluxes, which causes concentration polarization.

To circumvent these drawbacks, fluidized bed membrane reactors have been proposed for various reactions to extract gas (e.g. hydrogen) from or add gas (e.g. oxygen) to the reaction mixture, see Gallucci et al. (2008), Adris et al. (1997), Mleczko et al. (1996) and Hommel et al. (2012). Compared to packed bed membrane reactors, fluidized bed membrane reactors have better mixing properties, resulting in reduced mass transfer limitations towards the membranes. The hydrodynamics and mass transfer phenomena of the fluidized suspension can be strongly affected by the membrane configuration. Recently, the hydrodynamic implications of using membranes (i.e. without simulating actual mass transfer) in fluidized beds have been studied by e.g. De Jong et al. (2011, 2012a, 2012b), Dang et al. (2014), Tan et al. (2014), Roghair et al. (2014) and Medrano et al. (2015).

The present work will focus on the selective extraction of hydrogen from fluidized bed membrane reactors, with the goal to study and quantify mass transfer phenomena such as concentration polarization. A Two-Fluid Model (TFM) was used as the hydrodynamic framework, based on the OpenFOAM® *twoPhaseEulerFoam* solver (v.2.3.1). This solver has been extended with species balance equations and realistic membrane models to simulate the selective extraction dynamically, which is discussed in the following section.

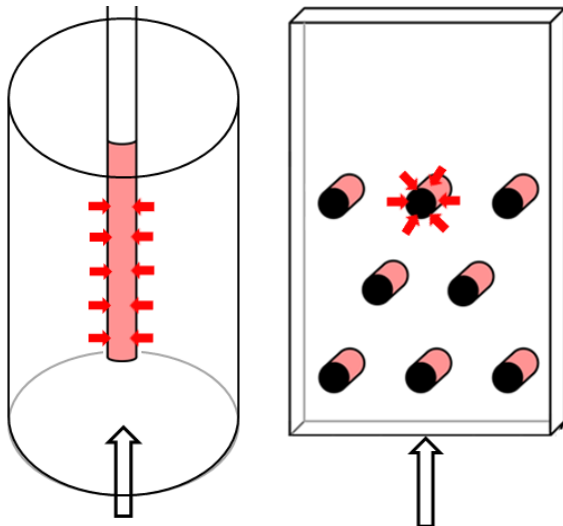


Figure 1: (left) Fluidized bed with vertically immersed membranes. (right) Fluidized bed with horizontally immersed membranes.

Next, the simulation setup of a fluidized bed with a vertically immersed membrane, and a fluidized bed with

horizontally immersed membranes (see **Figure 1**) are outlined, and the effects of the extraction on the mass transfer phenomena are discussed.

MODEL DESCRIPTION AND SETTINGS

Two-Fluid Model

A TFM considers the gas and solids phase as interpenetrating continua. The most important governing and constitutive equations are presented in equations 1 through 6. The continuity equations (1) of both gas and solids phase are the same. In case of extraction of a component via a membrane, a source term S should be added to the gas phase continuity equation. This will be elaborated in section about mass transfer and membranes. Compared to the Navier-Stokes equations of the gas phase (2), the Navier-Stokes equations for the solids phase (3) contain an additional solids pressure term p_s . For both phases a Newtonian stress tensor $\boldsymbol{\tau}$ is employed. The gas phase obeys the ideal gas law. Furthermore, the granular temperature equation (4) is solved, which incorporates the mean particle velocity and a superimposed fluctuating component, taking into account the vibrations of particles due to collisions.

$$\frac{\partial \alpha_i \rho_i}{\partial t} + \nabla \cdot (\alpha_i \rho_i \mathbf{u}_i) = S, \quad i = s, g \quad (1)$$

$$\begin{aligned} \frac{\partial \alpha_g \rho_g \mathbf{u}_g}{\partial t} + \nabla \cdot (\alpha_g \rho_g \mathbf{u}_g \mathbf{u}_g) \\ = -\nabla \cdot (\alpha_g \boldsymbol{\tau}_g) - \alpha_g \nabla p - \beta \cdot (\mathbf{u}_g - \mathbf{u}_s) + \alpha_g \rho_g \mathbf{g} \end{aligned} \quad (2)$$

$$\begin{aligned} \frac{\partial \alpha_s \rho_s \mathbf{u}_s}{\partial t} + \nabla \cdot (\alpha_s \rho_s \mathbf{u}_s \mathbf{u}_s) \\ = -\nabla \cdot (\alpha_s \boldsymbol{\tau}_s) - \alpha_s \nabla p - \nabla p_s + \beta \cdot (\mathbf{u}_g - \mathbf{u}_s) + \alpha_s \rho_s \mathbf{g} \end{aligned} \quad (3)$$

$$\begin{aligned} \frac{3}{2} \left(\frac{\partial (\alpha_s \rho_s \theta)}{\partial t} + \nabla \cdot (\alpha_s \rho_s \mathbf{u}_s \theta) \right) \\ = -(\mathbf{p}_s \mathbf{I} + \alpha_s \boldsymbol{\tau}_s) : \nabla \mathbf{u}_s + \nabla \cdot (\alpha_s \kappa_s \nabla \theta) - \gamma_s - 3\beta\theta \end{aligned} \quad (4)$$

The drag between the solids and the gas phase is modelled according to Gidaspow (1994), which combines the drag model of Ergun et al. (1949) and Wen et al. (1966). Ergun's model is valid for high solids hold-ups (20% and higher) and Wen's model is valid at lower solids hold-ups (below 20%). The drag coefficient C_d is determined based on the Reynolds particle number. The drag models are described in equations 5 until 9.

$$\beta = 150 \frac{\alpha_s^2 \mu_g}{\alpha_s d_p^2} + 1.75 \frac{\alpha_s \rho_g}{d_p} |\mathbf{u}_g - \mathbf{u}_s| \quad \text{for } \alpha_s \geq 0.20 \quad (5)$$

$$\beta = \frac{3}{4} C_d \frac{\alpha_s \alpha_g \rho_g}{d_p} |\mathbf{u}_g - \mathbf{u}_s| \alpha_g^{-2.65} \quad \text{for } \alpha_s < 0.20 \quad (6)$$

$$C_d = \frac{24}{\text{Re}_p} \left(1 + 0.15 \text{Re}_p^{0.687} \right) \quad \text{for } \text{Re}_p \leq 1000 \quad (7)$$

$$C_d = 0.44 \text{ for } Re_p > 1000 \quad (8)$$

$$Re_p = \alpha_g \frac{\rho_g d_p |\mathbf{u}_g - \mathbf{u}_s|}{\mu_g} \quad (9)$$

Kinetic Theory of Granular Flow

To simulate the rheological and collisional properties of the solids phase's continuum approximation more realistically, various KTGF closure equations are required. The closure equations used in this work are presented in Table 1.

Table 1: KTGF closures used for TFM simulations.

Quantity	Closure
Solids shear viscosity	Nieuwland (1996)
Solids bulk viscosity	Lun et al. (1984)
Solids pressure	Lun et al. (1984)
Frictional stress	Srivastava & Sundaresan (2003)
Conductivity of fluct. energy	Nieuwland (1996)
Radial distribution function	Ma & Ahmadi (1984)
Dissipation of granular energy	Nieuwland (1996)

Further details on the TFM-KTGF can be found a.o. in Lun et al. (1984), Kuipers et al. (1992), Gidaspo (1994), Van Wachem (2000), Rusche (2003) and Van Der Hoef et al. (2006). Details on the OpenFOAM® TFM can be found in Passalacqua et al. (2011) and Liu et al. (2014).

Mass transfer and membranes

The hydrogen mass balance was modelled via a transient convection-diffusion equation as shown in equation 10. Similar to Coroneo et al. (2009), the effect of the membranes on the system was taken into account via a source term, S_{H_2} , which was only applied to the computational cells adjacent to a membrane boundary. This way, a chemical component (i.e. hydrogen) can be removed from or added to the system. The value of the source term reflects the membrane flux through the boundary, which is obtained by using Sieverts' law, given in equation 11. The source term should also be added to the right side of the gas phase continuity equation, so the change in mass due to extraction or addition of a component is correctly taken into account, see equation 1.

$$\frac{\partial \alpha_g \rho_g Y_{H_2}}{\partial t} + \nabla \cdot (\alpha_g \rho_g \mathbf{u}_g Y_{H_2}) = \nabla \cdot (\alpha_g \rho_g D_{H_2} \nabla Y_{H_2}) + S_{H_2} \quad (10)$$

$$S_{H_2} = \frac{A}{V_c} Q_{pd} \cdot \left[(X_{H_2}^{ret} p_{tot})^n - (X_{H_2}^{perm} p_{tot})^n \right] \quad (11)$$

An often undiscussed topic in the literature on CFD simulations of membrane reactors is the extraction or addition of momentum from the system through the membrane, due to the extraction or addition of a chemical component. This could be an important topic for fluidized beds, because densified zones can form near the membranes and even the flow pattern of the solids may be affected. This has been shown by De Jong et al. (2011), who simulated the membranes as permeable walls. In the case of hydrogen extraction, the removal of momentum from the system is expected to have a limited effect due to hydrogen's low molecular weight. However, when

modelling extraction or addition of a component with a higher molecular weight, it may be significant.

A boundary condition was written which specifically applies a momentum flux, based on the magnitude of the extractive flux source term, on the membrane boundary. The boundary condition ultimately imposes a velocity normal to the membrane boundary (see equation 12).

$$u_m = \frac{S_{H_2} RT}{p M_{H_2}} \frac{V_c}{A_c} \quad (12)$$

Simulation settings and geometries

A fluidized bed reactor with a vertically immersed membrane was simulated and the results were compared with experiments. The experimental setup consists of a cylindrical fluidized bed reactor with a single submerged membrane in the centre of the reactor. This system was approximated by a 2D simulation. A sketch of the experimental set-up and the simulation are presented in Figure 2. To reduce simulation times, only the area next to the membrane was simulated. The hydrogen was extracted from the left boundary, to which the membrane velocity boundary condition described by equation 12 was applied. On the right boundary a no-slip condition was applied for the gas mixture. For the solids phase, a Johnson & Jackson partial slip boundary condition was applied on the left and right walls.

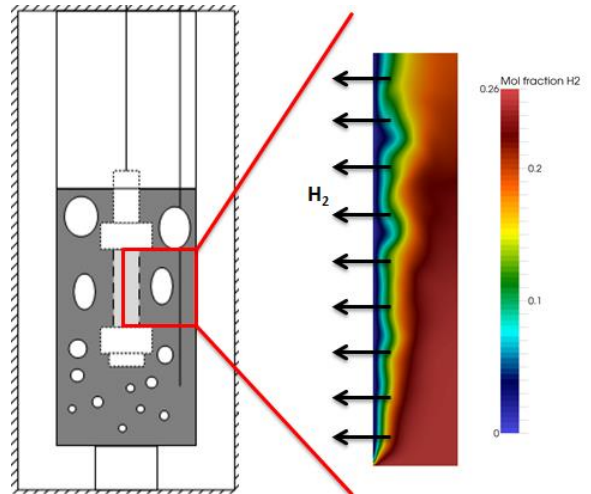


Figure 2: Vertical membrane set-up and its simulated 2 dimensional equivalent.

The settings for the vertical membrane simulations are presented in Table 2 and Table 3. The width is equal to the radius of the experimental reactor and the height is equal to the membrane's height. The bed was operated in the bubbling fluidization regime and the membrane parameters were obtained from experimental data. The simulations were performed at three different hydrogen molar fractions and four different outlet pressures.

For the horizontal membranes, the simulated geometry was also 2D. The dimensions and configuration of the membranes were equal to the experimental ones, see Figure 3. The settings of the horizontal membrane simulations are given in Table 4. Previous research has provided information on the system's hydrodynamics and can be consulted for details (Medrano et al. (2015)). The

hydrogen molar fraction at the inlet was set to 0.25 and the outlet pressure was set to 1.6 bar.

Table 2: Summary of TFM simulation settings for vertical membranes.

Quantity	Setting
Width (x)	0.0225 m
Height (y)	0.113 m
Number of cells width	40
Number of cells height	200
d_p	200 μm
ρ_p	1400 kg/m^3
u/u_{mf}	3.33
D	$1.0 \times 10^{-4} \text{ m}^2/\text{s}$
Q_{pd}	$4.3 \times 10^{-3} \text{ mol}/(\text{m}^2 \text{ s Pa}^n)$
n [-]	0.50
A_m	$1.836 \times 10^{-3} \text{ m}^2$
T	405 $^\circ\text{C}$
t_{sim}	15 s
Δt	$2 \times 10^{-5} \text{ s}$

Table 3: Summary of TFM simulation series for vertical membranes.

Molar fraction H_2 [-]	P_{outlet} [Pa]	P_{perm} [Pa]
0.10	1.5×10^5	0.01×10^5
0.25	1.6×10^5	
0.45	1.7×10^5	
	1.8×10^5	

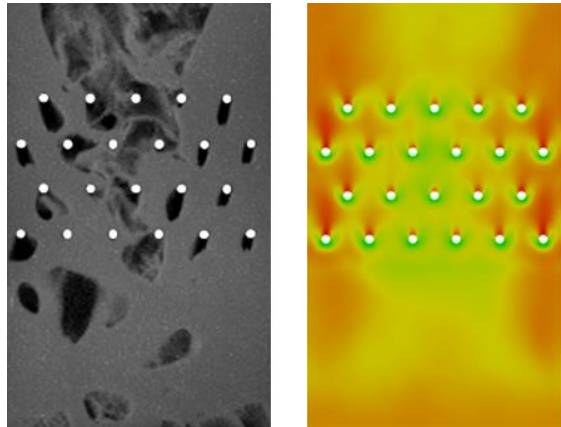


Figure 3: Horizontal membranes set-up for experiments (left) and simulations (right).

Table 4: Summary of TFM simulation settings for horizontal membranes.

Quantity	Setting
Width (x)	0.30 m
Height (y)	0.90 m
Number of cells width	60 (refined around memb.)
Number of cells height	180 (refined around memb.)
Number of membranes	22
Membrane diameter	9.6 mm
d_p	500 μm
ρ_p	2500 kg/m^3
u/u_{mf}	3.0
D	$1.3 \times 10^{-4} \text{ m}^2/\text{s}$
Q_{pd}	$3.32 \times 10^{-4} \text{ mol}/(\text{m}^2 \text{ s Pa}^n)$
n [-]	0.50
A_m	$9.953 \times 10^{-3} \text{ m}^2$ (22 memb.)
T	405 $^\circ\text{C}$
X_{H_2}	0.25
P_{outlet}	$1.6 \times 10^5 \text{ Pa}$
P_{perm}	0 Pa
t_{sim}	30 s
Δt	$2 \times 10^{-5} \text{ s}$

RESULTS

Vertical membranes

In Figure 4, membrane fluxes of experiments, results of a 1D Kunii-Levenspiel type model without taking concentration polarization into account (see Patil et al. (2005)) and the TFM results are presented. Concentration polarization has a pronounced effect on the membrane flux, which can be seen when comparing the experiments to the 1D model. The 1D model strongly overestimates the membrane flux due to the lack of a concentration polarization effect. The TFM, however, is capable of predicting the effect of concentration polarization correctly, hence the correct fluxes are obtained from the TFM simulations. The average deviation between experimental and simulated fluxes are found to be about 4%. The simplified 2D geometry already seems sufficient to predict the phenomena occurring in the cylindrical experimental set-up. Future simulations will be carried out in more complex (3D) geometries and at pressures outside of the experimental range, to study in more detail how this trend progresses. Furthermore, industrially relevant pressures and geometries can be explored.

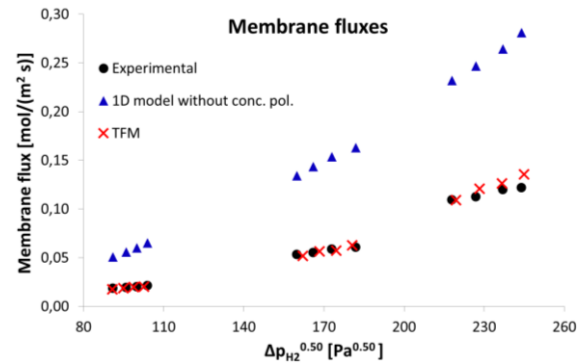


Figure 4: Membrane fluxes of the experiments, 1D simulation without taking concentration polarization into account and Two Fluid Model.

One of the biggest advantages of the TFM simulations is that data can be obtained which is experimentally often inaccessible or can only be obtained by using intrusive measurement techniques. Figure 5 displays the time-averaged hydrogen molar fraction profiles using a fluidization gas consisting of 25% hydrogen and 75% nitrogen at 1.5 bar total pressure. The profiles show the extent of concentration polarization at various axial positions. In the present work, the width of the concentration polarization zone is defined as the width where 95% of the bulk hydrogen concentration is reached. The polarization zone width increases with height, because fresh hydrogen is supplied faster to the bottom of the membrane than to the top. On average, the polarization zone width is constant at about one third of the total height. On average, 50-60% of the reactor width is polarized (about 0.013 m).

The polarization zone widths presented in Figure 6 show no clear trend over the four simulated pressures. However, the pressure range is insufficiently extensive, thus simulations at other pressures should be performed to study this in more detail. The average polarization decreases with increasing hydrogen molar fraction. This is in line with expectations, because when measuring

systems with pure hydrogen, no concentration polarization is observed and membrane fluxes are significantly higher compared to fluxes at binary gas mixtures. For larger scale systems it is expected that concentration polarization will occur as well, however, it will most probably be less significant than for the laboratory scale system in this study.

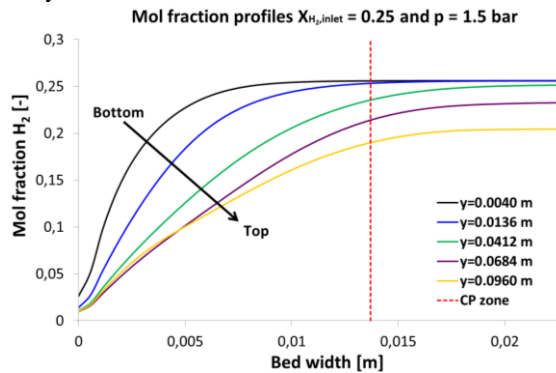


Figure 5: Hydrogen molar fraction profiles of versus bed width at various bed heights (y). The red dotted line is the average polarization zone width.

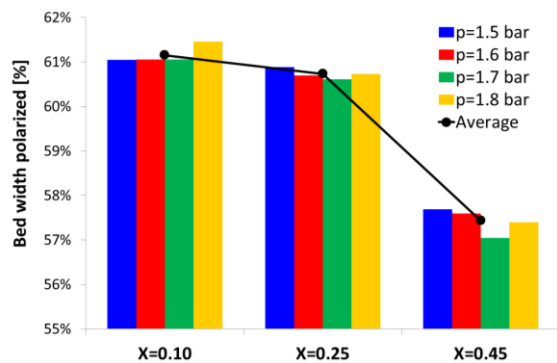


Figure 6: Concentration polarization zone widths at various injected hydrogen molar fractions and pressures.

Horizontal membranes

Horizontal membranes have various hydrodynamic effects on the reactor. Apart from their effect on the solids circulation pattern (see Medrano et al. (2015)), densified zones occur on top of the membranes and gas pockets (solids free regions that do not rise and are attached to the membranes) mostly appear under the membranes. In Figure 7 (top) the time-averaged solids hold-up is displayed, which indicates that over time most of the densified zones and gas pockets appear near the fluidized bed walls.

The mass transfer phenomena near horizontal membranes show that reduced hydrogen concentrations, and thus reduced membrane fluxes, are found around the membranes near the column walls, see Figure 7 (bottom). The most direct explanation for this decline in hydrogen concentration is that the densified zones and gas pockets affect the mass transfer from the emulsion phase to the membrane. More precisely, densified zones, gas pockets, concentration polarization and concentration reduction tend to occur where the solids flow downwards most of the time. These observations are in line with expectations of the hydrodynamic study by Medrano et al. (2015). More simulations and more detailed analyses have to be

performed in order to quantify and further explain the phenomena occurring in fluidized bed membrane reactors. In the near future, an extension of our experimental work (Dang et al. 2013) on the use of infrared cameras to measure concentration fields in fluidized beds will be combined with TFM simulations to understand the details of these systems.

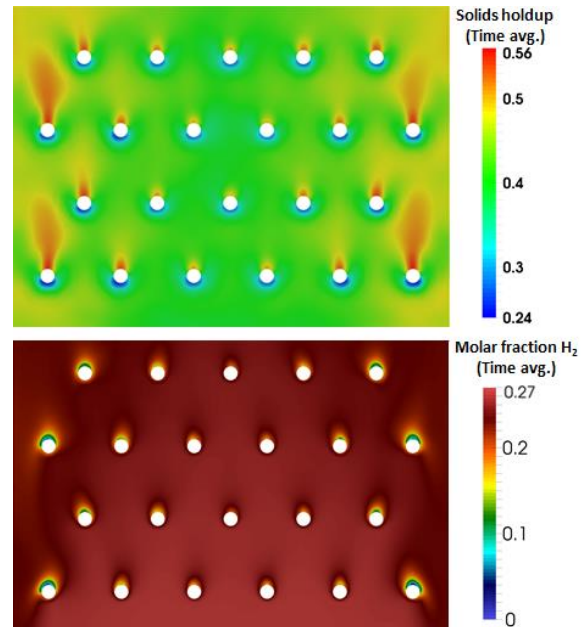


Figure 7: (Top) Time-averaged solids hold-up near the horizontal membranes. (Bottom) Time-averaged hydrogen molar fractions near the horizontal membranes.

CONCLUSION

Two Fluid Model simulations of fluidized bed membrane reactors with vertically and horizontally immersed membranes have been performed in order to quantify and understand mass transfer phenomena occurring in these systems. The model's results were compared to experimental work.

The model was able to predict experimental fluxes of the vertical membrane set-up within 4%. The concentration polarization zone width increases with increasing axial positions. The average polarization zone width was 50-60% of the reactor width. On average, the polarization zone width is stable at about one third of the total height. The average polarization zone width decreases with increasing hydrogen molar fractions.

In fluidized beds with horizontal membranes densified zones occur on top of and gas pockets occur under the membranes. The locations in the reactor where densified zones and gas pockets are most observed also show the lowest hydrogen concentrations near the membranes, and thus also the lowest membrane fluxes.

Future work will focus on the detailed comparison of vertical and horizontal membranes. The advantages and disadvantages of using vertical and horizontal membranes will be looked at, and simulations at industrially relevant conditions, scales and geometries will be performed. Furthermore, the TFM will be extended to be able to simulate multi-species mass transfer and reactive flows.

ACKNOWLEDGEMENTS

The authors are grateful to the Dutch Technology Foundation (STW) and the Netherlands Organization for Scientific Research (NWO) for their financial support through the VIDI project ClingCO₂, project number 12365.

REFERENCES

ADRIIS, A.M., LIM, C.J. and GRACE, J.R., (1994), "The fluidized bed membrane reactor system: a pilot scale experimental study", *Chem. Eng. Sc.*, **49**, 5833-5843.

CORONEO, M., MONTANTE, G., CATALANO, J. and PAGLIANTI, A., (2009), "Modelling the effect of operating conditions on hydrodynamics and mass transfer in a Pd-Ag membrane module for H₂ purification", *J. Memb. Sc.*, **343**, 34-41.

DANG, T.Y.N., GALLUCCI, F. and VAN SINT ANNALAND, M., (2014), "Micro-structured fluidized bed membrane reactors: solids circulation and densified zones distribution", *Chem. Eng. J.*, **239**, 42-52.

ERGUN, S. and ORNING, A., (1949), "Fluid flow through randomly packed columns and fluidized beds", *Ind. Eng. Chem.*, **41**, 1179-1184.

GALLUCCI, F., VAN SINT ANNALAND, M. and KUIPERS, J.A.M., (2008), "Autothermal reforming of methane with integrated CO₂ capture in a novel fluidized bed membrane reactor. Part 1: experimental demonstration", *Top. Catal.*, **51**, 133-145.

GALLUCCI, F., VAN SINT ANNALAND, M. and KUIPERS, J.A.M., (2010), "Theoretical comparison of packed bed and fluidized bed membrane reactors for methane reforming", *Int. J. Hydrogen Energy*, **35**, 7142-7150.

GIDASPOW, D., (1994), "Multiphase flow and fluidization: continuum and kinetic theory descriptions", *Academic Press Inc.*

HAN, C. and HARRISON, D.P., (1994), "Simultaneous shift reaction and carbon dioxide separation for the direct production of hydrogen", *Chem. Eng. Sc.*, **49**, 5875-5883.

HOMMEL, R., Cloete, S. and AMINI, S., (2012), "Numerical investigations to quantify the effect of horizontal membranes on the performance of a fluidized bed reactor", *Int. J. Chem. React. Eng.*, **10**.

DE JONG, J., VAN SINT ANNALAND, M. and KUIPERS, J.A.M., (2011), "Experimental study on the effects of gas permeation through flat membranes on the hydrodynamics in membrane-assisted fluidized beds", *Chem. Eng. Sc.*, **66**, 2398-2408.

DE JONG, J., VAN SINT ANNALAND, M. and KUIPERS, J.A.M., (2012a), "Membrane-assisted fluidized beds - part 2: numerical study on the hydrodynamics around immersed gas-permeating membrane", *Chem. Eng. Sc.*, **84**, 822-833.

DE JONG, J., DANG, T.Y.N., VAN SINT ANNALAND, M. and KUIPERS, J.A.M., (2012b), "Comparison of a discrete particle model and a two-fluid model to experiments of a fluidized bed with flat membranes", *Powder Technol.*, **230**, 93-105.

KUIPERS, J.A.M., VAN DUIN, K., VAN BECKUM and F., VAN SWAAIJ, W., (1992), "A numerical model of gas-fluidized beds", *Chem. Eng. Sci.*, **47**, 1913-1924.

KUNII, D. and LEVENSPIEL, O., (1991), "Fluidization Engineering", *Butterworth-Heinemann*.

LIU, Y. and HINRICHSSEN, O., (2014), "CFD modeling of bubbling fluidized beds using OpenFOAM®: Model

validation and comparison of TVD differencing schemes", *Comp. & Chem. Eng.*, **69**, 75-88.

LUN, C., SAVAGE, L., JEFFREY, D., and CHEPURNIY, N., (1984), "Kinetic theories for granular flow: inelastic particles in Couette flow and slightly inelastic particles in a general flowfield", *J. Fluid Mech.*, **140**, 223-256.

MEDRANO, J.A., SPALLINA, V., VAN SINT ANNALAND, M. and GALLUCCI, F., (2014), "Thermodynamic analysis of a membrane-assisted chemical looping reforming reactor concept for combined H₂ production and CO₂ capture", *Int. J. Hydrogen Energy*, **39**, 4725-4738.

MEDRANO, J.A., VONCKEN, R.J.W., ROGHAI, I., GALLUCCI, F. and VAN SINT ANNALAND, M., (2015), "On the effect of gas pockets surrounding membranes in fluidized bed membrane reactors: An experimental and numerical study", *Chem. Eng. J.*, doi:10.1016/j.cej.2015.04.007.

MLECZKO, L., OSTROWSKI, T. and WURZEL, T., (1996), "A fluidised-bed membrane reactor for the catalytic partial oxidation of methane to synthesis gas", *Chem. Eng. Sc.*, **51**, 3187-3192.

PASSALACQUA, A. and FOX, R.O., (2011), "Implementation of an iterative solution procedure for multi-fluid gas-particle flow models on unstructured grids", *Powder Technol.*, **213**, 174-187.

PATIL, C.S., VAN SINT ANNALAND, M. and KUIPERS, J.A.M., (2005), "Design of a novel autothermal membrane-assisted fluidized-bed reactor for the production of ultrapure hydrogen from methane", *Ind. Chem. Eng. Res.*, **44**, 9502-9512.

ROGHAI, I., GALLUCCI, F. and VAN SINT ANNALAND, M., (2014), "Novel developments in fluidized bed membrane reactor technology", *Modeling and simulation of heterogeneous catalytic processes / Ed. A.G. Dixon (Elsevier)*, **45**, 159-283.

RUSCHE, H., (2002), "Computational fluid dynamics of dispersed two-phase flows at high phase fractions", PhD thesis, *University of London*.

TAN, L., ROGHAI, I. and VAN SINT ANNALAND, M., (2014), "Simulation study on the effect of gas permeation on the hydrodynamic characteristics of membrane-assisted micro fluidized beds", *Appl. Math. Model.*, **38**, 4291-4307.

TIEMERSMA, T., PATIL, C.S., VAN SINT ANNALAND, M. and KUIPERS, J.A.M., (2006), "Modelling of packed bed membrane reactors for autothermal production of ultrapure hydrogen", *Chem. Eng. Sc.*, **61**, 1602-1616.

TSOTSIS, T.T., CHAMPAGNIE, A.M., VASILEIADIS, S.P., ZIACA, Z.D. and MINET, R.G., (1992), "Packed bed catalytic membrane reactors", *Chem. Eng. Sc.*, **47**, 2903-2908.

VAN DER HOEF, M.A., YE, M., VAN SINT ANNALAND, M., ANDREWS IV, A.T., SUNDARESAN, S. and KUIPERS, J.A.M., (2006) "Multi-scale modeling of gas-fluidized beds", *Adv. Chem. Eng.*, **31**, 65-149.

VAN WACHEM, B., (2000), "Derivation, implementation, and validation of computer simulation models for gas-solid fluidized beds", PhD thesis, Delft University of Technology.

WEN, C. and YU, Y., (1966) "A generalized method for predicting the minimum fluidization velocity" *AICHEJ.* **12**, 610-612.